IOP Conf. Series: Journal of Physics: Conf. Series **838** (2017) 012009 doi:10.1088/1742-6596/838/1/012009

Dynamics of nanomaterials released from polymer composites in the pelletizing process

Nobuyuki Kato[1], Yasuto Matsui [2] and Minoru Yoneda[1]
(1) Graduate School of Engineering, Kyoto University, Katsura, Nishikyoku, Kyoto, 615-8540, Japan; (2) Agency for Health, Safety and Environment, Kyoto University, Yoshidahonmachi, Sakyoku, Kyoto, 606-8501, Japan
E-mail: katoh@risk.env.kyoto-u.ac.jp

Abstract. Measures against exposure to carbon nanotubes (CNT) are necessary, especially in workplaces that handle nanomaterials, because adverse health effects are a concern. This study focuses on the dynamics of CNT released from CNT/polymer composites during the pelletizing process at a pilot factory. It is difficult to identify CNT and the base resin. By characterizing the possibility of separating CNT from the composite with a kinetic weighting coefficient, estimation can be carried out using a Computational Fluid Dynamics (CFD) simulation. The mass concentration of black carbon and the particle number concentration by diameter were measured using two different measurement apparatuses. The simulation results were then compared to the measured data. The model was verified by the correlation between the simulation and measured results. The model provided a strong correlation, indicating that the dynamics of CNT and the base resin released from the polymer composite can be simulated. It is expected that the model using the CFD simulation can be applied to the occupational health field.

1. Introduction

The applications of nanomaterials in various fields have vastly increased in the past decade. On the one hand, the small size of nanomaterials which at least in one dimension are smaller than 100 nm allows for new functions. On the other hand, many reports have indicated negative impacts on experimental animals and cells [1–4]. For example, composite materials with carbon nanotubes (CNT) are being produced because adding CNT to a base material to a concentration of several percentages realizes new functions such as conductivity. However, the health effects of CNT remain a concern. Therefore, measures against exposure are necessary, especially in workplaces that handle nanomaterials.

Numerous exposure assessments in workplaces handling nanomaterials have been reported. A survey has been conducted in a CNT pilot factory. However, identifying and assessing the exposure of scattered CNT in pilot factories that deal with CNT/polymer composite resins are difficult by thermal carbon analysis using NIOSH 5040 [5] due to the fact that carbon is already in the air and CNT is composed of carbon resin materials.

Elemental analysis using metal impurities in CNT as a marker is being attempted to identify CNT [6–9]. At CNT/polymer composite pilot factories, CNT goes through the following process. First, CNT materials are repacked into smaller bags (repacking), which are fed into an extruder (feeding). Then the resin and CNT are extruded (extruding). After the composite resin is cooled, it is cut into pellets (pelletizing). During pelletizing, the cutting process has been reported to produce a momentary high concentration, but the specific release has yet to be resolved.

This study focuses on the pelletizing process. By characterizing the possibility of separating CNT from the base resin with a kinetic weighting coefficient, estimations can be conducted using Computational Fluid Dynamics (CFD) simulations.

Measurements were conducted using a light scattering dust counter (LSDC) for area sampling of dust, black carbon monitoring (BCM) to measure the black carbon concentration, and an optical particle sizer (OPS) to measure the suspended particulate matter concentrations (size range: 0.3–10 μm). The rate of CNT released from the composite resin was calculated using the advection-diffusion model, revealing the dynamics of CNT.

2. Methodology

2.1. Sample design

Figure 1 depicts the factory layout. During working hours, all doors are closed. To measure the airborne particulate matter concentrations, LSDCs (Model LD-3, SHIBATA) were placed at six different sampling points (No.1–6) for 25 minutes. Measurements were taken every second. The mass concentration conversion coefficient (K factor) was set to 0.001 mg/m^3/cpm. K factor was based on the reference value. Measurements taken at points No. 2, 4, and 5 were during the pelletizing process.

In addition, the particle concentrations during each process was measured close to the processes (sampling points No. 7–9 in Figure 1) using an OPS (Model 3330, TSI Inc, size range 300 nm–10 μm). The OPS obtained the particle concentrations at a rate of 10 sec/scan. The equipment except in the fume hood was set at 1.1 m above the ground, which is the height of the breathing area.

The mass concentrations of airborne CNT was measured using BCM (Model AE51, AethLabs) at sampling points No. 10–12 in Figure 1. The running condition of BCM was at a flow rate of 0.1 L/min and a time interval of 60 seconds. To compare the base line of the ambient concentration before and after pelletizing, this study focused on the pelletizing process.

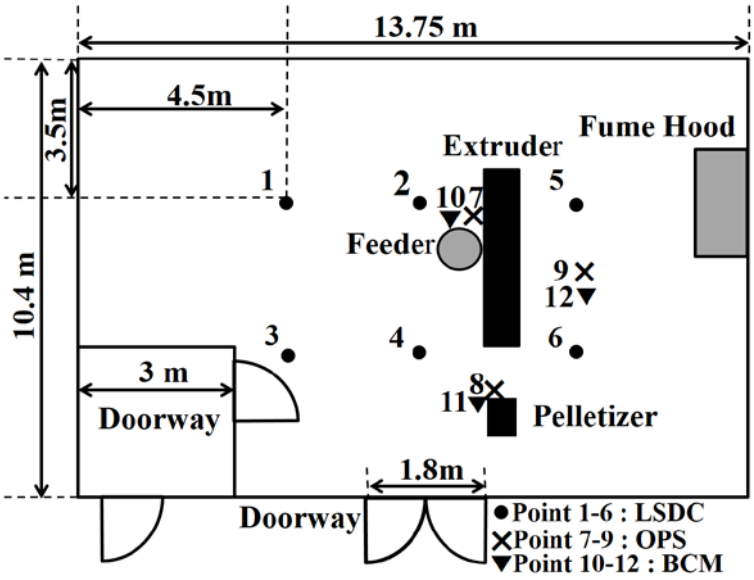

Figure 1. Outline of the factory showing approximate positions of the processes and mobile measurement locations (1–12).

2.2. CFD simulation calculation conditions

A computation mesh was created using a mesh generator. The temperature of the extruder was set rather high (280°C) for calculation purposes. Figure 2 shows the calculation area.

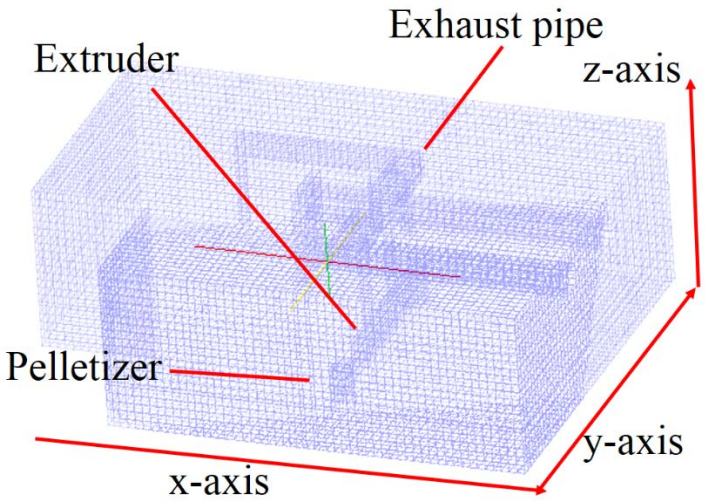

Figure 2. Surface mesh of the extruder and the pelletizer in the manufacturing factory.

The mesh size was selected to reduce the calculation costs. However, dynamics analysis was simulated using 20-cm intervals (69×52×42 [cell]). In this study, the simulation was conducted using the free model (OpenFOAM [10]). As for the flow field, the differential equation was discretized and then the 3D field was decided by steady-state analysis. The fluid was assumed to be a Newtonian. The equations of OpenFOAM, continuity equation, Navier-Stokes equation, and energy transfer equation (Equation 1–3) were used. The concentration field was analyzed by time integrating the scalar transfer equation that does not consider interactions. In addition to the aforementioned equations, the ideal gas equation was also used.

$$\nabla \cdot (\rho u) = 0 \tag{1}$$

$$\frac{\partial \rho u}{\partial t} + \nabla \cdot (\rho u u) = -\nabla p - \nabla \cdot \left[\mu \left\{\nabla u + (\nabla u)^T\right\}\right] - \nabla\left(\frac{2}{3}\mu \nabla \cdot u\right) \tag{2}$$

$$\frac{\partial \rho E}{\partial t} + \nabla \cdot (\rho E u) = -\nabla \cdot (\rho u) + \nabla \cdot (k \nabla T) \tag{3}$$

E is the total energy per mass, k is the thermal conductivity, and T is the absolute temperature. Here, the gravity term is ignored. The total energy E is the sum of the internal energy and the kinetic energy. The gravity buoyancy can be considered under the assumption that a hydrostatic equilibrium is possible using the Boussinesq approximation. The gravity term is calculated using Equation 4.

$$\rho g = \left\{1 - \beta(T - T_0)\right\}\rho_0 g \tag{4}$$

ρ_0 : basic density, T_0 : basic temperature, β: coefficient of cubic expansion.

For the turbulent model in this survey, Reynolds-averaged Navier-Stoles (RANS) was used. The RANS model comes in various forms. To confirm the mesh quality in obtaining y+ from the wall, the most stable potential fluid was achieved around 100–150. Therefore, by defining the Reynolds stress using the eddy viscosity, the standard k-ε model modeled by the wall-law logarithmic space was selected. Shown below is the equation.

$$\frac{\partial \bar{u}}{\partial t} + \bar{u} \cdot \nabla \bar{u} = -\nabla \bar{p} - \nabla \cdot (\nu_{eff} \nabla \bar{u}) \tag{5}$$

where ν_{eff} is the coefficient of the eddy viscosity, whereby ν_t is added to ν, which is the constant of the turbulent term. $\bar{u}$ in the equation is the mean velocity of the flow (Equation 5).

Constants k and ε obtained from the standard k-ε model were derived from the Equations 6 and 7. K is the turbulent energy and ε is the energy disposal rate. Constants k and ε were obtained from the standard k-ε model. For the standard k-ε model, the eddy viscosity coefficient was calculated by obtaining k and ε when solving the two transfer equation modeled by two variables (k and ε).

$$\frac{\partial k}{\partial t} + \frac{\partial \bar{u}_i k}{\partial x_i} = S - \frac{\partial}{\partial x_i}(\nu + \frac{\nu_t}{\sigma_k}\frac{\partial \varepsilon}{\partial x_i}) - \varepsilon \tag{6}$$

$$\frac{\partial \varepsilon}{\partial t} + \frac{\partial \bar{u}_i \varepsilon}{\partial x_i} = C_{\varepsilon 1}\frac{\varepsilon}{k}S + \frac{\partial}{\partial x_i}(\nu + \frac{\nu_t}{\sigma_k}\frac{\partial \varepsilon}{\partial x_i}) - C_{\varepsilon 2}\rho\frac{\varepsilon^2}{k} \tag{7}$$

Each coefficient is defined by Launder-Spalding (1974). C_μ= 0.09, $C_{\varepsilon 1}$=1.44, $C_{\varepsilon 2}$=1.92, σ_k =1.0, σ_ε = 1.0.

The initial values (k and ε) were derived from Equations 8 and 9.

$$k = \frac{3}{2}(UI)^2 \tag{8}$$

$$\varepsilon = \frac{C_\mu^{0.75} k^{1.5}}{L_m} \tag{9}$$

I is the turbulent magnitude. In this survey, the fluctuation value of 0.08, which was measured with an anemometer, was used as the UI value. The default value C_μ of the standard k-ε model (0.09) was used. L_m is the mixing-length. For the representative length L, which is the length that receives the greatest impact, 7% was selected. In this survey, the width of the extruder, which is the turbulent source, was used as the representative length.

Using these values, the turbulent viscosity coefficient μ_t and turbulent heat diffusion coefficient α_t were determined using Equations 10 and 11. In the case of air, the experimental value was around 0.9 at the wall boundary. In this model, the calculation was carried out with P_{rt}＝0.85.

$$\mu_t = \rho C_\mu \frac{k^2}{\varepsilon} \tag{10}$$

$$\alpha_t = \frac{\mu_t}{p_{rt}} \tag{11}$$

The scalar transfer equation is as shown below (Equation 12). S is the source term.

$$\frac{\partial \phi}{\partial t} + u \cdot \nabla \phi = \nabla \cdot (D \nabla \phi) + S \tag{12}$$

In addition, the equilibrium velocity of the normal force and gravity was obtained as the terminal velocity to model the characteristic of the particulate matter (Equation 13).

$$v_t = \frac{\rho_{\mathrm{P}} d_{\mathrm{ve}}{}^2 g C_C(d_{\mathrm{ve}})}{18 \mu \chi} \tag{13}$$

Here, d_{ve} is the equivalent volume diameter, g is the gravitational acceleration, μ is the viscosity, and χ is the kinetic weighting coefficient. Spherical shape is 1. C_C is the Cunningham weighting factor, and is shown as the Knudsen number (Kn) function (Equation 14). Kn (= 2λ /d) can be represented as the rate between the molecular mean free path λ and the diameter d. For λ, the value adjusted to the temperature of the experiment condition was used. This velocity was added to u in Equation 12 in the virtual down direction.

$$C_C = 1 + 1.257\,Kn + 0.400\,Kn \exp\left(\frac{-1.10}{Kn}\right) \tag{14}$$

The diffusion coefficient D is represented by the Stokes-Einstein equation (Equation 15)

$$D = \frac{k T C_C(d_{\mathrm{ve}})}{3\pi \mu \chi d_{\mathrm{ve}}} \tag{15}$$

Here, k is the Boltzmann constant and T is the absolute temperature. This D was used as the constant D in Equation 12. For stable state conditions, the SIMPLE method was used. The provisional velocity was calculated by the semi-discrete scheme of the motion equation. After this, the pressure equation was solved from the provisional velocity. Subsequently, the velocity was updated using that pressure. This process was repeated until residual value was minimized.

Table 1 shows the calculation conditions. All factory doors were closed. The internal current was simulated from the thermal convection produced by the Extruder.

As previously mentioned, the pelletizing process was first conducted with a resin to investigate the concentration distribution. By focusing on this process and the steady flow, the concentration of CNT and resin released from the pelletizer were simulated. Because the operation time of the resin was 30 minutes, the simulation of the concentration transfer was carried out for 30 minutes. For the real-time measurements, the measurement time of LSDC was considered and the gradient of the increasing function over 20 minutes from the start to before the concentration rapidly increases was compared to the simulation value. In addition, the correlation coefficient between measurement value and simulation value was obtained.

With the CNT aspect ratio used for this process and the bulk density, two kinds of simulations were conducted. For an aspect ratio of 50, χ = 2.0. Using the aerodynamics diameter calculated based on the catalog data of CNT used in the study, χ = 3.5. These two values were used. For the resin value, 1.04 g/m^3 was used according to the physical properties, and a bulk density of 0.12 g/m^3 was used for CNT.

Considering the shape, the terminal velocity was calculated. For OPS, to match the units of the calculation, the number concentration was transferred to the mass concentration as 1 mg/cm^3. Table 1 shows the initial calculation conditions.

Finally, the CNT containing rate was assumed to be 5.0%. Then, the simulation result of the CNT model released from the pelletizer was compared to measured value from BCM. For each material (CNT of shape χ = 2.0, 3.5 and resin), different simulation scenarios were prepared using nine types of diameters (50 nm, 100 nm, 300 nm, 500 nm, 1 μm, 2 μm, 4 μm, 7 μm, 10 μm). The simulation scenarios were selected based on the measurement apparatus and analytical purpose.

Table 1. Calculation conditions.

	Parameter
Calculation area	69×52×42 [grid]
Discrete method	Finite volume method
Initial air condition (U, p)	U = 0 [m/s](air velocity) p = 0.1[Mpa]
Initial temperature	Air = 293.15[K], Extruder = 553.15 [K]
Initial condition (k,ε)	k = 0.0096, ε = 0.0003
Turbulent kinematic velocity	ν_t = 0.0268 [m^2/s]
Boundary condition	Uwall = 0 [m/s] Pressure gradient = 0
Prandtl number	Pr_t = 0.85

3. Results

Figure 3 depicts the calculation result of the steady flow with the simple method, and shows the magnitude of the potential flow in the center and its vector flow.

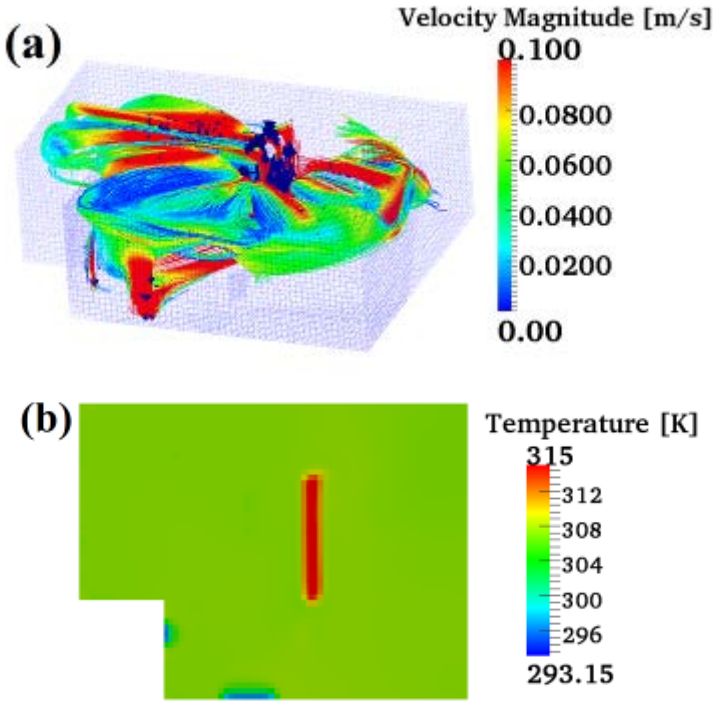

Figure 3. Velocity magnitude destribution of the air stream line and the temperature desutribution at the breathing area height. (a) Air stream line velocity and vector. (b) Temperature cross section of the breathing line.

Due to thermal convection, the flow moves upwards and around the room in general. In addition, by measuring the temperature distribution at points 7–9 at the start of the pelletizing process, the mean temperature from a thermometer at a breathing height is 34.8°C, which approximately matches the calculated temperatures of 35.8°C, 34.3°C, and 35.4°C (Figure 4b). From these results, the mass advection-diffusion simulation from the pelletizer was simulated by assuming that the simulation of the potential flow is reasonable.

Next, to grasp the trend of the mass diffusion model, the simulated calculations at Points 1–9 in Figure 1 were conducted. CNT (χ = 2.0, 3.5) and resin were generated every second from the pelletizer. To determine the distribution difference between each particulate matter, the distribution was calculated every 30 minutes. Figures 4 and 5 show the simulation results. The calculated concentration was normalized in order to obtain the tendency of the difference of diameters without depending on generating quantity of particulate matters.

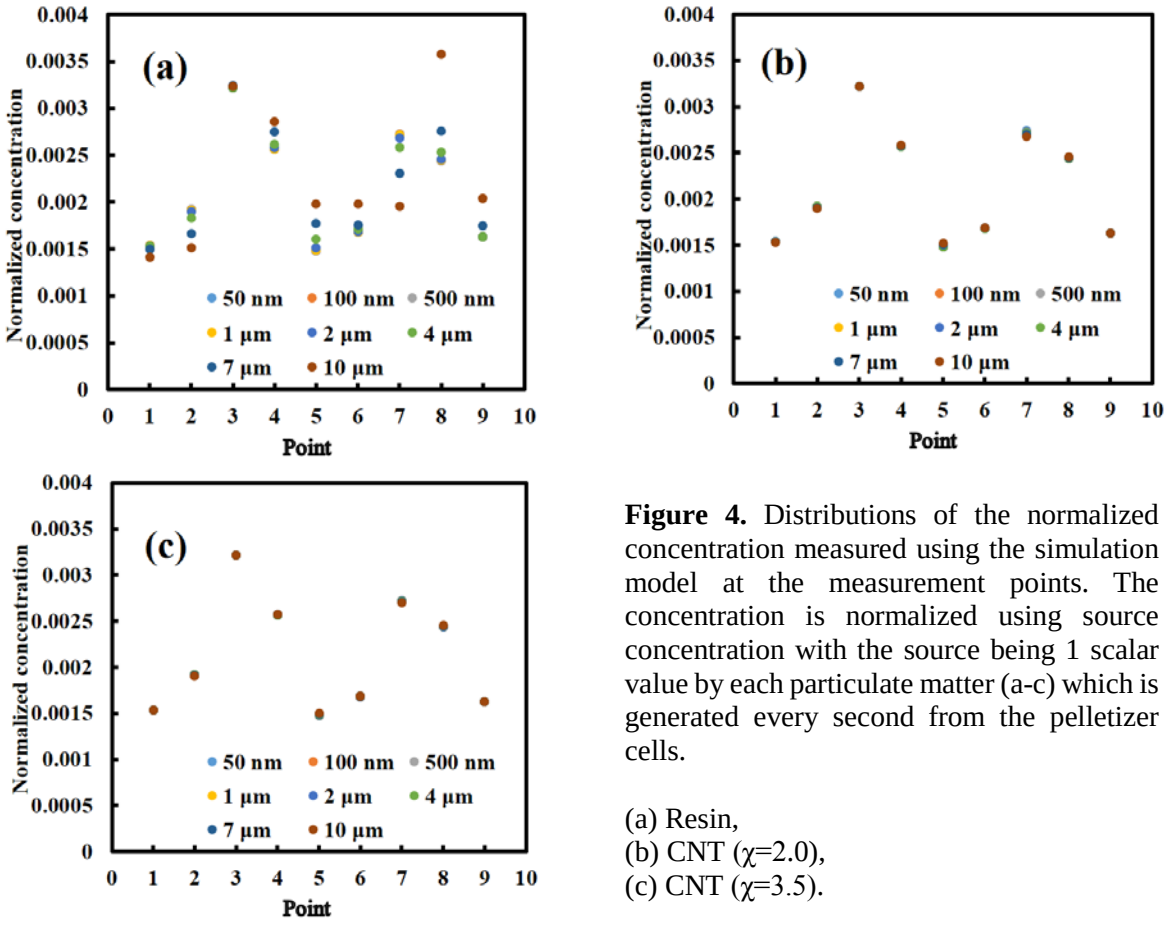

Figure 4. Distributions of the normalized concentration measured using the simulation model at the measurement points. The concentration is normalized using source concentration with the source being 1 scalar value by each particulate matter (a-c) which is generated every second from the pelletizer cells.

(a) Resin,
(b) CNT (χ=2.0),
(c) CNT (χ=3.5).

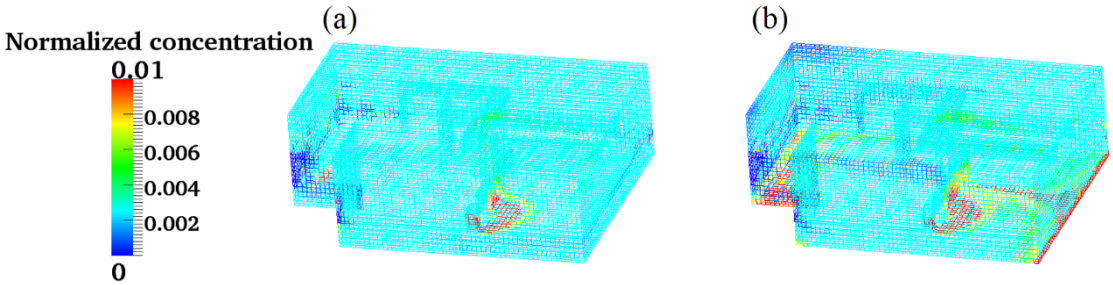

Figure 5. Resin normalized concentration distributions after 30 min. (a) Resin diameter is 500 nm and (b) Resin diameter is 10 µm.

Regarding the Resin particles, some integrations of measurement points are easier for heavier particles, while other integrations are easier for lighter particles. However, in terms of CNT, the dispersion is independent of the diameter and the kinetic weighting coefficient.

Next, to assess the simulation model, the correlation coefficient of the time series data was obtained by time series data using LSDC and simulations at the measurement points. Figure 6 and Table 2 show the simulation results.

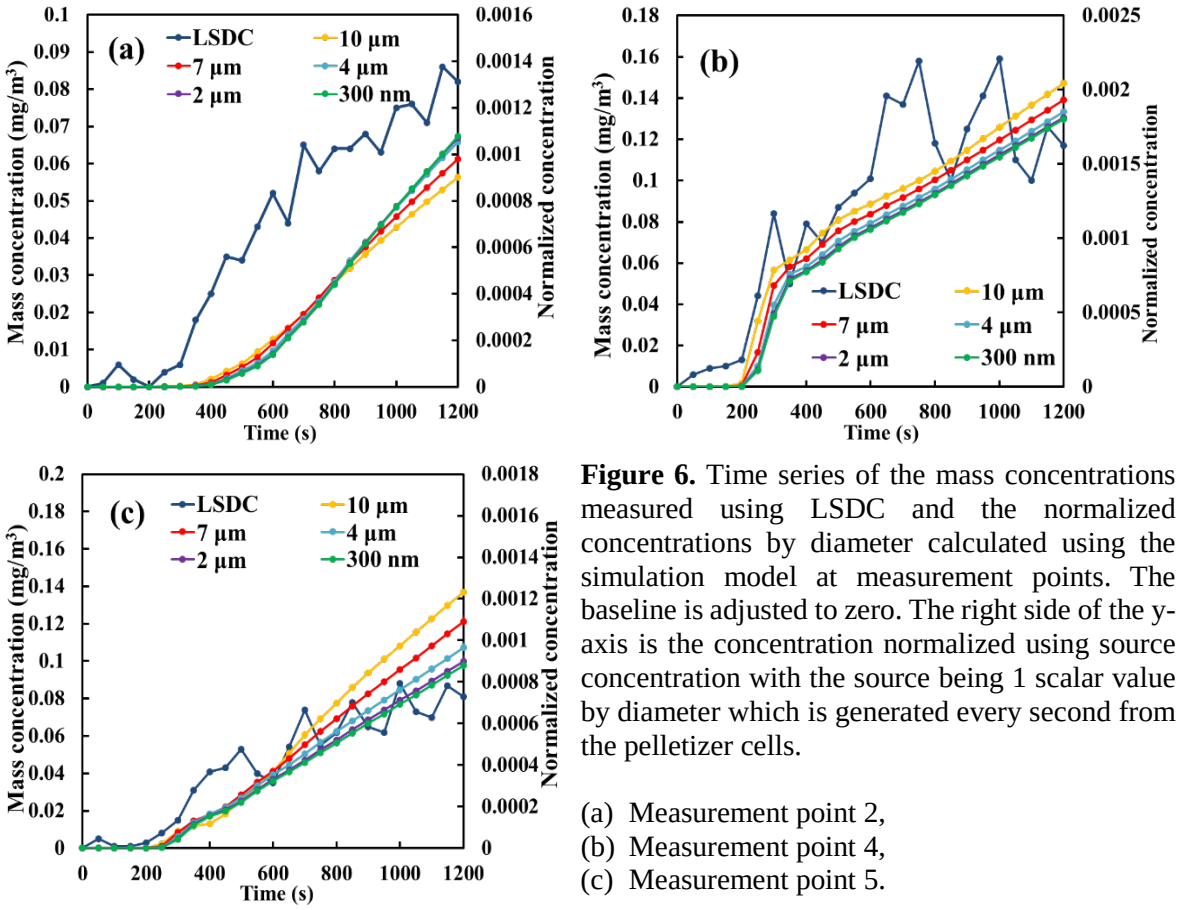

Figure 6. Time series of the mass concentrations measured using LSDC and the normalized concentrations by diameter calculated using the simulation model at measurement points. The baseline is adjusted to zero. The right side of the y-axis is the concentration normalized using source concentration with the source being 1 scalar value by diameter which is generated every second from the pelletizer cells.

(a) Measurement point 2,
(b) Measurement point 4,
(c) Measurement point 5.

As a result, at each measurement point, the time of increase in concentrations measured using LSDC, corresponds reasonably well with that of increase in concentrations calculated using the model. Moreover, gradients of the concentration curve measured at the point 4 and 5 correspond well with the concentrations calculated using the model.

Table 2. Correlation coefficients of the LSDC concentration data and the simulation concentrations data.

Measurement point	Resin diameter	Correlation coefficient
2	300 nm	0.88
4	300 nm	0.88
5	300 nm	0.93

LSDC was calibrated using stearic acid particles (diameter range: 300 nm). Table 2 shows the results calculated by 300 nm. As a result, the correlation coefficients indicate that all the points show a strong correlation. In addition, at Point 5, which is relatively far, a particle of size 300 µm has the strongest correlation because of the light weight.

Next, the correlation coefficients of the time series data were obtained by time series data using OPS and a simulation at points of measurement. Figure 7 and Table 3 show the simulation results.

The particle number concentrations measured using OPS were converted to the mass concentrations by the assumed density (1 g/cm^3). The particles assumed to be spherical for the mass determination.

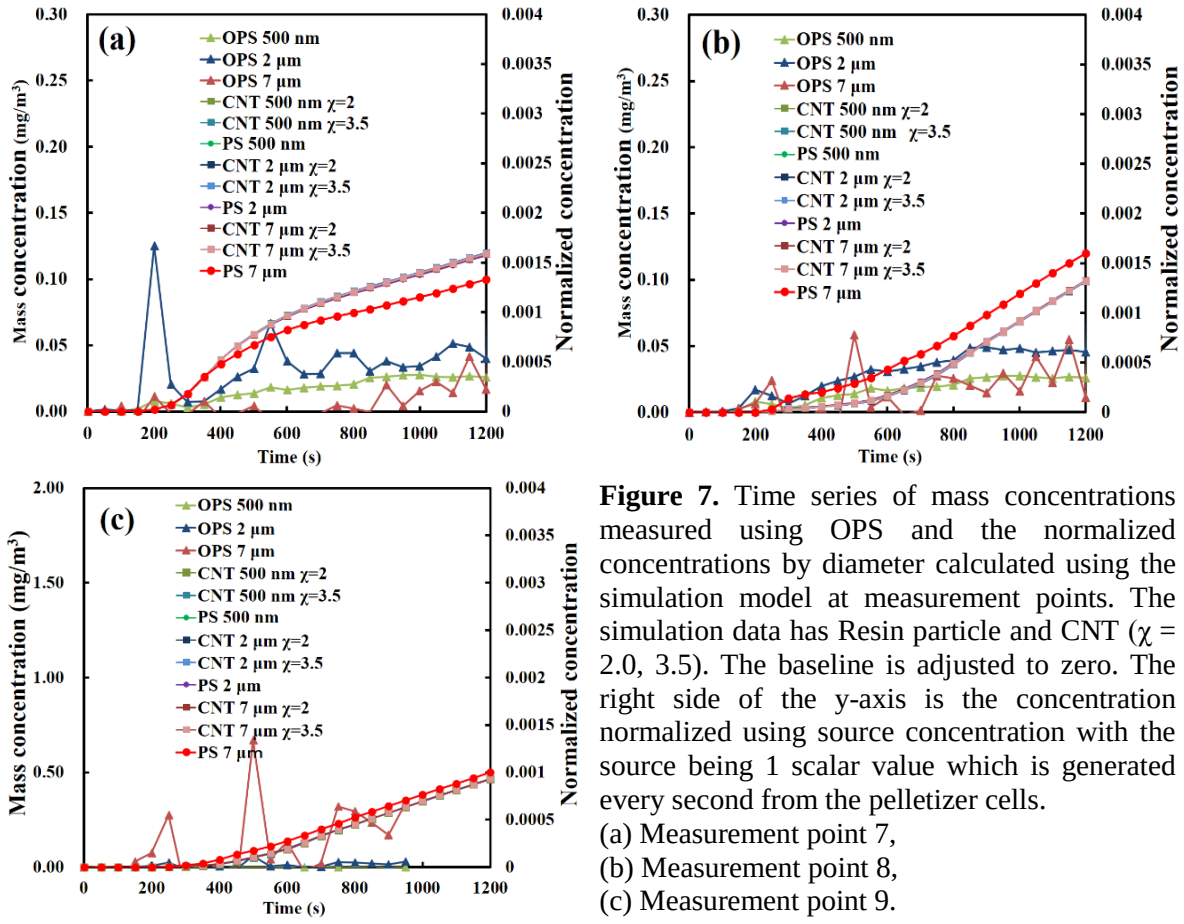

Figure 7. Time series of mass concentrations measured using OPS and the normalized concentrations by diameter calculated using the simulation model at measurement points. The simulation data has Resin particle and CNT (χ = 2.0, 3.5). The baseline is adjusted to zero. The right side of the y-axis is the concentration normalized using source concentration with the source being 1 scalar value which is generated every second from the pelletizer cells.
(a) Measurement point 7,
(b) Measurement point 8,
(c) Measurement point 9.

Table 3. Correlation coefficients of the OPS concentration data and the simulation concentration data.

Measurement point	Diameter	Material and shape	Correlation coefficient
7	500 nm	Resin	0.98
7	500 nm	CNT χ=2	0.98
7	500 nm	CNT χ=3.5	0.98
7	2 µm	Resin	0.98
7	2 µm	CNT χ=2	0.98
7	2 µm	CNT χ=3.5	0.98
7	7 µm	Resin	0.97
7	7 µm	CNT χ=2	0.98
7	7 µm	CNT χ=3.5	0.98
8	500 nm	Resin	0.85
8	500 nm	CNT χ=2	0.85
8	500 nm	CNT χ=3.5	0.85
8	2 µm	Resin	0.86
8	2 µm	CNT χ=2	0.85
8	2 µm	CNT χ=3.5	0.85
8	7 µm	Resin	0.91

8	7 μm	CNT χ=2	0.85
8	7 μm	CNT χ=3.5	0.85
9	500 nm	Resin	-0.28
9	500 nm	CNT χ=2	-0.28
9	500 nm	CNT χ=3.5	-0.28
9	2 μm	Resin	0.47
9	2 μm	CNT χ=2	0.47
9	2 μm	CNT χ=3.5	0.47
9	7 μm	Resin	0.48
9	7 μm	CNT χ=2	0.47
9	7 μm	CNT χ=3.5	0.47

Point 7 around the feeder shows a stronger correlation with CNT. Point 8 around the pelletizer shows a stronger correlation with resin, confirming that particles with a spherical shape and higher density are detected. At Point 9, 500-nm particles show a negative correlation, suggesting that the influence of particulate matter rather than the materials released from the pellet during the pelleting process is detected. Spherically shaped particles with higher densities and diameters greater than 2 μm show a stronger correlation at Point 9.

Finally, the correlation coefficient of the time series data was obtained by time series data using the BCM and CNT simulation data converted into 5 wt. % at measurement points. Figure 8 and Table 4 show the simulation results.

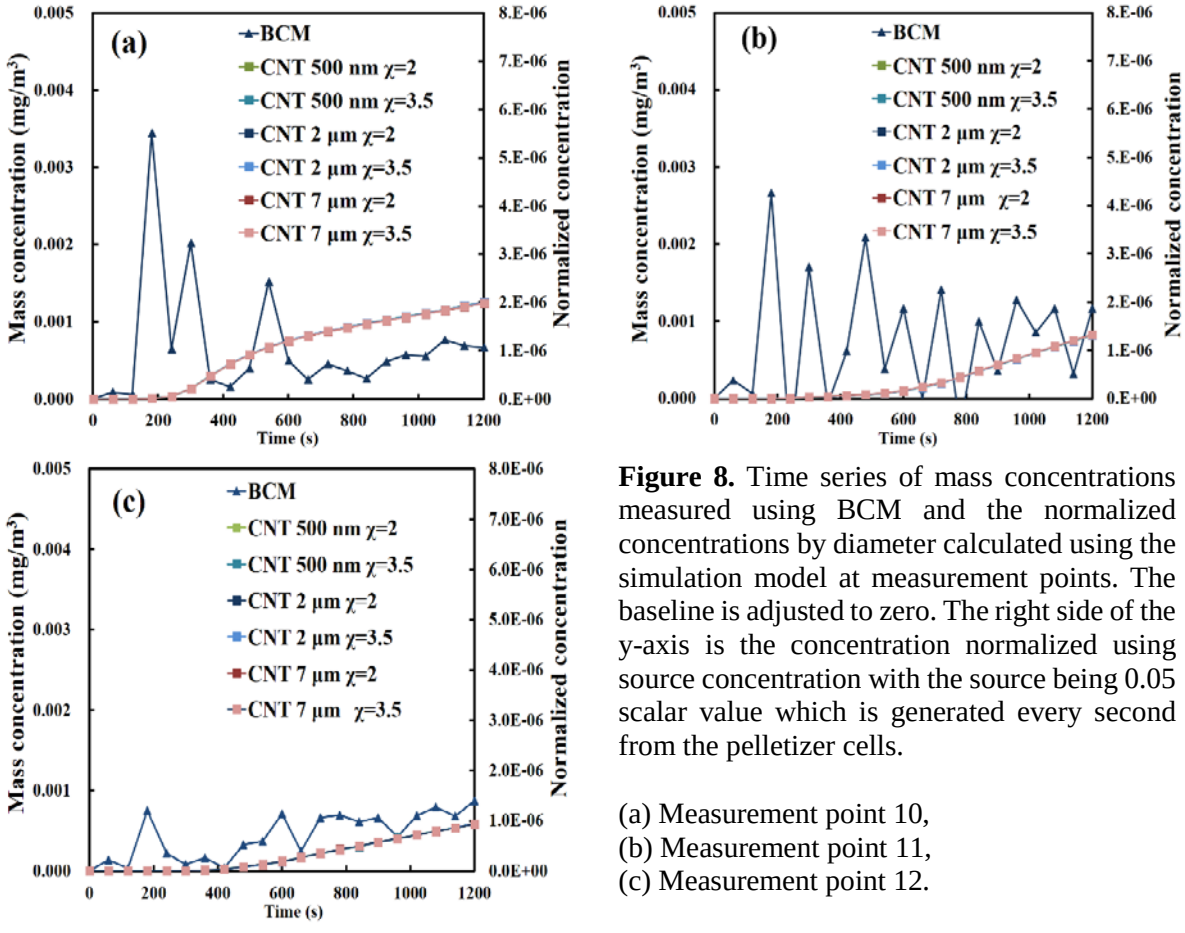

Figure 8. Time series of mass concentrations measured using BCM and the normalized concentrations by diameter calculated using the simulation model at measurement points. The baseline is adjusted to zero. The right side of the y-axis is the concentration normalized using source concentration with the source being 0.05 scalar value which is generated every second from the pelletizer cells.

(a) Measurement point 10,
(b) Measurement point 11,
(c) Measurement point 12.

Table 4. Correlation coefficients of the BCM concentration data and the simulation concentration data.

Measurement point	Diameter	Shape	Correlation coefficient
10	500 nm	CNT $\chi = 2$	-0.197
10	500 nm	CNT $\chi = 3.5$	-0.197
10	2 μm	CNT $\chi = 2$	-0.197
10	2 μm	CNT $\chi = 3.5$	-0.197
10	7 μm	CNT $\chi = 2$	-0.197
10	7 μm	CNT $\chi = 3.5$	-0.197
11	500 nm	CNT $\chi = 2$	0.056
11	500 nm	CNT $\chi = 3.5$	0.056
11	2 μm	CNT $\chi = 2$	0.056
11	2 μm	CNT $\chi = 3.5$	0.056
11	7 μm	CNT $\chi = 2$	0.056
11	7 μm	CNT $\chi = 3.5$	0.056
12	500 nm	CNT $\chi = 2$	0.736
12	500 nm	CNT $\chi = 3.5$	0.736
12	2 μm	CNT $\chi = 2$	0.736
12	2 μm	CNT $\chi = 3.5$	0.736
12	7 μm	CNT $\chi = 2$	0.737
12	7 μm	CNT $\chi = 3.5$	0.737

Point 10 and 11are not correlated with CNT. However, Point 12 shows a stronger correlation with CNT.

4. Conclusion

By modelling CNT and resin with a kinetic weighting coefficient, the dynamics of CNT and resin released from the composite during the pelletizing process was verified. The higher the kinetic weighting coefficient was, the weaker the dependence on the diameter. Since the terminal velocity was slower, the particles easily floated. Comparative simulations of the diameters and materials revealed that the resin particles dispersed in relation to the diameter and the kinetic weighting coefficient. However, no such dispersion dependence existed for CNT. The times series concentrations of LSDC and the simulation data as well as OPS data were strongly correlated.

The measurement points closer to the pelletizer showed a strong correlation with larger particles, whereas smaller particles showed the strongest correlation with measurement points at a relatively far distance. In contrast, BCM showed a negative correlation around the feeder and no correlation around the pelletizer. Since a local ventilation was used during the feeding process, it was difficult to measure the higher CNT concentration continuously.

However, when extruding and pelletizing started, a sharp peak in the OPS data with a diameter below a few micrometers temporarily appeared. Since the BC concentration scale is smaller than the OPS concentration scale, BCM was considered to be more sensitive to residual dust than OPS. It was assumed that the simulation result and BCM data were not correlated at point 10 and point 11[11].

Point 12, which was relatively far from the extruder and pelletizer, showed a strong correlation with the simulation results. In particular, there was a stronger correlation with larger particles as well as the OPS data. Moreover, the maximum correlation was detected in the resin particle data. Therefore, there is a low probability that free and isolated CNT were released from CNT/polymer composites during the pelletizing process.

Next, the reproducibility of mass advection-diffusion modeling in the workplace was verified. The measured concentrations showed an increasing function, but the gradient of the curve at 800 seconds decreased. Our simulation model has yet to reproduce this trend. Since the peak of concentrations measured using OPS with a different diameter was approximately consistent in Figure 7, the aggregation in air was not estimated in this study. It was assumed that by extruding continuously, the real temperature field was separated from the temperature field obtained using steady-state analysis. Drying the surrounding air showed the terminal velocity of airborne particulate matter was slower than in the moist environment, allowing the particles to float easily. Other possible assumptions include the deposition of particulate matter on the factory surfaces (exhaust pipe, wall etc.) and instability of the pelletizing amount. To reproduce such conditions, it is necessary to model the interaction of evaporation, which requires a precise mesh of the factory surroundings.

However, this study revealed that the simple model is sufficient to determine the correlation. In conclusion, this model can be used to simulate dispersion of particulate matter in workplaces.

Acknowledgements

This study is based on the results obtained from a project commissioned by the New Energy and Industrial Technology Development Organization (NEDO).

References

[1] Brown DM, Wilson MR, MacNee W et al. 2001 *Size-dependent proinflammatory effects of ultrafine polystyrene particles. A role for surface area and oxidative stress in the enhanced activity of ultrafines. Toxicol.Appl.Pharmacol* **175**: 191-199.

[2] Lam CW, James J J, McCluskey R et al. 2004 *Pulmonary toxicity of single-wall CNT in Mice 7 and 90 days after intratracheal instillation. Toxicol Sci* **77**: 126-134.

[3] Takagi A, Hirose A, Nishimura T et al. 2008 *Induction of mesothelioma in p53 ± mouse by intraperitoneal application of multi-wall carbon nanotube. J Toxicol Sci* **33**: 105-116.

[4] Poland CA, Duffin R, Kinloch I et al. 2008 *Carbon nanotubes introduced into the abdominal cavity of mice show asbestos-like pathogenicity in a pilot study. Nat Nanotechnol* **3**: 328-333.

[5] NIOSH: current intelligence bulletin 65 2013 Occupational exposure to carbon nanotubes and nanofibers. Cincinati, Ohio: US Department of Health and Human Services Centers for Disease Control and Prevention, National Institute for Occupational Safety and Health; Publication No.2013-145.

[6] Birch ME, Ku BK, Evans DE, Ruda-Eberenz TA . 2011 *Exposure and emissions monitoring during carbon nanofiber production-Part 1: elemental carbon and iron-soot aerocols. The Annals of Occupational Hygiene* **55**: 1016-1136.

[7] Maynard AD, Baron PA, Foley M, Shvedova AA, Kisin ER, Castranova V. 2004 *Exposure to carbon nanotube material: aerosol release during the handling of unrefined single-walled carbon nanotube material. Journal of Tocicology and Environmental Health* Part A **67**: 87-107.

[8] Rasmussen PE, Jayawardene I, Gardner HD, Chenier M, Levesque C, Niu J. 2013 *Metal impurities provide useful tracers for identifying exposures to airborne single-wall carbon nanotube paritcles released from work-related processes. Journal of Physics: Conference Series* **429**: 012007.

[9] Reed RB, Goodwin DG, Marsh KL, Capracotta SS, Higgins CP, Fairbrother DH, Ranville JF. 2013 *Detection of single walled carbon nanotubes by monitoring embeded metals. Environmental Science: Processes & Impacts* **15**: 204-213.

[10] OpenFoam http://www.openfoam.com/

[11] Kuhlbusch TA, Fissan H. 2006 *Particle characteristics in the reactor and pelletizing areas of carbon black production. J Occup Environ Hyg* **3**: 558-567.